mean onset age for the family, a combined standard deviation from the onset ages in all families (8.62 years), and an ultimate penetrance of 100%. For the phenocopy correction model, lod scores were determined by an age-dependent penetrance model with a phenocopy correction that assumes a cumulative normal age-of-onset function with a mean of 110 years and a standard deviation of 14 years (*12*). Possible heterogeneity was examined with the admixture test [S. E. Hodge, C. E. Anderson, K. Neiswanger, R. S. Sparkes, D. L. Rimoin, *ibid.* **35**, 1139 (1983)].

18. Unless otherwise noted, published allele frequencies are from the Genome Database.
19. J. Ott, *Am. J. Hum. Genet.* **51**, 283 (1992).
20. Marker order for some loci was from G. Gyapay *et al.*, *Nat. Genet.* **7**, 246 (1994); this order with centimorgan (sex-averaged) distances is D1S238–4–D1S422–4–D1S412–7–D1S306–6–D1S249–7–D1S245–1–D1S205–2–D1S425/D1S217–6–D1S229–1–D1S227–4–D1S439/D1S213/D1S479–3–D1S225–2–D1S459–2–D1S446–4–D1S235. As part of this study, additional mapping of six loci was performed with the complete CEPH mapping panel (40 families) and the computer program CRIMAP [E. R. Lander and P. Green, *Proc. Natl. Acad. Sci. U.S.A.* **84**, 2363, (1987)]; the order was D1S229–5.7–D1S320–2.6–D1S213–1–D1S479/D1S439–5.4–D1S103.
21. Initial power analysis of the families (which did not include the neuropathologic samples) indicated that with a reasonably polymorphic marker [PIC = 0.7; D. Botstein, R. L. White, M. Skolnick, R. W. Davies, *Am. J. Hum. Genet.* **32**, 314 (1980)], at $\theta = 0.05$, the mean $Z_{max} = 2.91$ with a maximum expected lod score of 7.55, and at $\theta = 0.1$, these lod scores would be 1.8 and 6.25, respectively. These lod scores are somewhat less than the 4.40 actually obtained, but as the power analysis did not assume the availability of the neuropathologic samples, such a result was expected.
22. Control allele frequencies for D1S479 were determined by allele counting. Frequencies for grandparents of members of pedigrees from the Centre d'Etude du Polymorphisme Humain (CEPH) (244 control chromosomes), all the VG subjects (affecteds, at-risk, and spouses; 254 chromosomes), affected VG subjects (74 chromosomes), and VG spouses (32 chromosomes) are respectively: 102 bp, 0.013, 0.012, 0.0, and 0.063; 104 bp, 0.029, 0.012, 0.00, and 0.031; 106 bp, 0.074, 0.055, 0.027, and 0.063; 108 bp, 0.013, 0.004, 0.0, and 0.031; 110 bp, 0.344, 0.343, 0.257, and 0.438; 112 bp, 0.041, 0.165, 0.31, and 0.031; 114 bp, 0.033, 0.055, 0.054, and 0.0; 116 bp, 0.307, 0.263, 0.243, and 0.219; 118 bp, 0.049, 0.008, 0.014, and 0.031; 120 bp, 0.066, 0.067, 0.054, and 0.094; 122 bp, 0.013, 0.004, 0.014, and 0.0; 124 bp, 0.012, 0.012, 0.027, and 0.0; 126 bp, 0.008, 0.0, 0.0, and 0.0.
23. P. Margaritte, C. Bonaiti-Pellie, M.-C. King, F. Clerget-Darpoux, *Am. J. Hum. Genet.* **50**, 1231 (1992).
24. J. Ott, *Analysis of Human Genetic Linkage* (Johns Hopkins Univ. Press, Baltimore, 1991); L. L. Cavalli-Sforza and M.-C. King, *Am. J. Hum. Genet.* **38**, 599 (1986).
25. Lod scores computed using the phenocopy correction model for D1S479 were $Z_{max} = 4.60$ ($\hat{\theta} = 0.10$) and $Z_{max} = 6.51$ ($\hat{\theta} = 0.08$) with the VG and control allele frequency for the 112-bp allele, respectively. Under this model, the maximum D1S479 lod score for a single family, the R family, was 2.95 ($\hat{\theta} = 0.09$) using the control allele frequency for the D1S479 112-bp allele. For other markers, maximum lod scores under the phenocopy correction model were as follows: D1S227, $Z_{max} = 0.92$, $\hat{\theta} = 0.20$; D1S213, $Z_{max} = 0.27$, $\hat{\theta} = 0.20$; D1S439, $Z_{max} = 3.13$, $\hat{\theta} = 0.15$; D1S225, $Z_{max} = 1.40$, $\hat{\theta} = 0.23$; D1S459, $Z_{max} = 0.27$, $\hat{\theta} = 0.30$; D1S103, $Z_{max} = 2.58$, $\hat{\theta} = 0.06$.
26. Multipoint linkage analysis was not performed because of the extraordinary computer time necessary with traditional methods. Alternatives based on simulation methods are under development [A. Kong, N. Cox, M. Frigge, M. Irwin, *Genet. Epidemiol.* **10**, 483 (1993); S. Lin, E. Thompson, E. M. Wijsman, *IMA J. Math. Appl. Med. Biol.* **10**, 1 (1993); S. Lin, E. M. Wijsman *Am. J. Hum. Genet.* **55**, A40 (1994)]; however, such methods cannot yet accommodate age-dependent reduced penetrance, and thus cannot be used for AD linkage analysis.
27. X.-D. Cai, T. E. Golde, S. G. Younkin, *Science* **259**, 514 (1993); M. Citron *et al.*, *Nature* **360**, 672 (1992); M. Citron *et al.*, *Proc. Natl. Acad. Sci. U.S.A.* **91**, 11993 (1994); N. Suzuki *et al.*, *Science* **264**, 1336 (1994); A. Tamaoka *et al.*, *J. Biol. Chem.* **269**, 32721 (1994).
28. D. Games *et al.*, *Nature* **373**, 523 (1995).
29. Supported by grants from the National Institute on Aging for the Alzheimer's Disease Research Center at the University of Washington (AG05136, G. M. Martin, director), the National Center for Human Genome Research (HG00835), Veterans Affairs Research Funds, an National Research Studies Alzheimer's post-doctoral fellowship (F32 AG05635), the American Health Assistance Foundation, and the American Physicians Fellowship. We thank D. Nochlin, M. Sumi, M. Ball, and G. Glenner for neuropathologic characterization of many of the families, E. Loomis and H. Utsugi for technical help, H. Lipe and T. Lampe for obtaining blood samples and medical records, D. Breiter for assistance with computations, and M. Boehnke and A. Motulsky for reading the manuscript prior to publication. Informed consent was obtained from each subject or next of kin with approval of the University of Washington Human Subjects Review Committee. We also thank the many family members who generously cooperated in this study, the American Historical Society of Germans from Russia, and T. Kloberdanz, G. Miner, and R. Cook-Deegan.

2 June 1995; accepted 14 July 1995

Candidate Gene for the Chromosome 1 Familial Alzheimer's Disease Locus

Ephrat Levy-Lahad,* Wilma Wasco,* Parvoneh Poorkaj, Donna M. Romano, Junko Oshima, Warren H. Pettingell, Chang-en Yu, Paul D. Jondro, Stephen D. Schmidt, Kai Wang, Annette C. Crowley, Ying-Hui Fu, Suzanne Y. Guenette, David Galas, Ellen Nemens, Ellen M. Wijsman, Thomas D. Bird, Gerard D. Schellenberg,† Rudolph E. Tanzi

A candidate gene for the chromosome 1 Alzheimer's disease (AD) locus was identified (*STM2*). The predicted amino acid sequence for *STM2* is homologous to that of the recently cloned chromosome 14 AD gene (S182). A point mutation in *STM2*, resulting in the substitution of an isoleucine for an asparagine (N141I), was identified in affected people from Volga German AD kindreds. This N141I mutation occurs at an amino acid residue that is conserved in human S182 and in the mouse S182 homolog. The presence of missense mutations in AD subjects in two highly similar genes strongly supports the hypothesis that mutations in both are pathogenic.

Alzheimer's disease is the most common cause of dementia in the elderly. The pathogenic pathway leading to neurodegeneration and AD is not well understood. However, at least some forms of the disease have a genetic etiology. For autosomal dominant, early-onset (<65 years) AD, causative mutations have been identified in the amyloid precursor protein (APP) gene on chromosome 21 (*1*), and mutations that segregate with familial AD (FAD) have been identified in S182, a strong candidate gene for the chromosome 14 AD3 locus (*2*). In addition to these major gene effects, the ϵ4 allele of the apolipoprotein E (APOE) gene modifies the risk of developing some forms of AD, possibly by lowering the age of onset (*3*). A third autosomal dominant locus, responsible for AD in the Volga German (VG) kindreds, has been recently localized to chromosome 1q31-42 (*4*). Identification of this locus was complicated by the overlap in the ages of onset of the affected VG subjects with late-onset AD, which is a common disease; thus, potential phenocopies, presumably a result of etiologic (genetic and nongenetic) heterogeneity, were observed among the affected VG subjects (*4*).

Nine VG families were used in this study (Fig. 1). The ancestors of these families immigrated from the Hesse region of Germany to Russia in the 1760s and subsequently to the United States at the turn of the 20th century (*5*). The families were ascertained as part of our larger genetic linkage studies because they contained multiple cases of autopsy-documented AD occurring in two or more generations. Families with both early- and late-onset AD cases were included. Detailed clinical, neuropathologic, and genetic studies of these families have been published elsewhere (*6*, *7*).

E. Levy-Lahad, P. Poorkaj, J. Oshima, C.-E. Yu, E. Nemens, G. D. Schellenberg, Geriatric Research, Education, and Clinical Center (182B), Veterans Affairs Medical Center, 1660 South Columbian Way, Seattle, WA 98108, USA.
W. Wasco, D. M. Romano, W. H. Pettingell, P. D. Jondro, S. D. Schmidt, A. C. Crowley, S. Y. Guenette, R. E. Tanzi, Genetics and Aging Unit, Massachusetts General Hospital, Charlestown, MA 02129, USA.
K. Wang, Y.-H. Fu, D. Galas, Darwin Molecular, Bothell, WA 98021, USA.
E. M. Wijsman, Division of Medical Genetics, Department of Medicine and Department of Biostatistics, University of Washington, Seattle, WA 98195, USA.
T. D. Bird, Division of Neurology, Veterans Affairs Medical Center, Seattle, WA 98108, USA.

*These authors contributed equally to this work.
†To whom correspondence should be addressed.

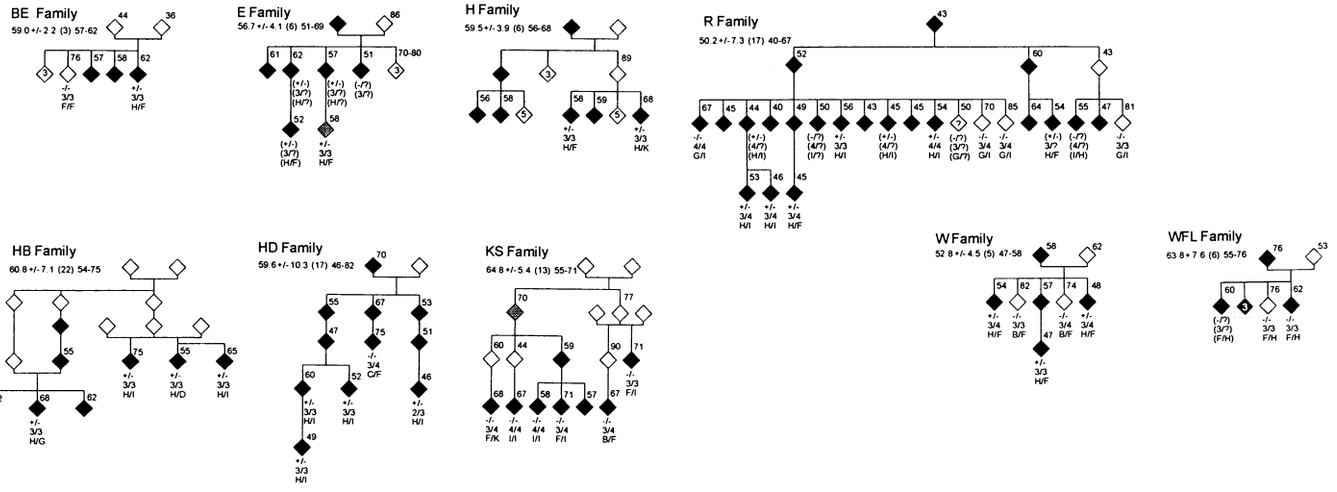

Fig. 1. Segregation of N141I, D1S479, and APOE genotypes in VG pedigrees. Genotypes given beneath the symbols (top to bottom) are as follows; N141I status (+ indicates the presence of the mutation); APOE genotypes (2, 3, and 4 are the ε2, ε3, and ε4 alleles, respectively); and D1S479 genotypes (A, 126 bp, B, 124 bp; C, 122 bp; D, 120 bp; E, 118 bp; F, 116 bp; G, 114 bp; H, 112 bp; I, 110 bp; J, 108 bp; K, 106 bp; L, 104 bp; and M, 102 bp). The allele frequency for the 112-bp allele is 0.041 in Caucasian controls and 0.031 in VG spouses (*4*). Genotypes in parentheses were deduced from spouse and offspring genotypes. The number above and to the right of the family members is the age of onset for affected subjects, the current age for living subjects, or the age at death for unaffected subjects. For each pedigree, the mean age of onset ± the standard deviation, the number of affected subjects used to compute the mean in parentheses, and the age of onset range is given. For the WFL pedigree, one affected subject had the 112-bp D1S479 allele. However, this subject's haplotype, constructed from surrounding markers, was not consistent with the haplotype segregating with AD in the other pedigrees (*4*). Solid symbols represent affected subjects, open symbols unaffected subjects, and stippled symbols possible AD subjects. The pedigrees have been altered to protect confidentiality, and not all subjects genotyped are shown. Also, to further disguise the pedigrees, living and deceased individuals are not distinguished, and some of the family members shown were not available for sampling.

Two strategies were used to identify the AD chromosome 1 gene. The first approach was to use yeast artificial chromosomes (YACs) to clone the chromosome 1 AD locus region, as defined by linkage analysis (*4*). A total of 60 YACs between flanking markers D1S229 and D1S103 were isolated (*8*) with the eventual goal of identifying transcripts as new genes from this region. The second strategy was to test for mutations in known candidate genes in this interval. The first candidate tested was a gene at 1q31 that encodes cathepsin E (*9*), a protease that is present in elevated amounts in the brains of AD patients (*10*), and is potentially capable of cleaving APP at the β-secretase site. No mutations were identified in the open reading frame of this gene. The second candidate tested was identified as a homolog to S182, the candidate AD3 gene (*2*). A 475-bp expressed sequence tagged (EST) sequence (T03796) was identified in the translated EST database and was 80.5% identical in amino acid sequence to S182. A rodent-human somatic cell hybrid panel was used to map this EST to chromosome 1 (*11*). T03796 was found on a single chromosome 1 YAC (921D12) (Fig. 2A) that also contained D1S439 and D1S479 (*12*). Previous work showed that

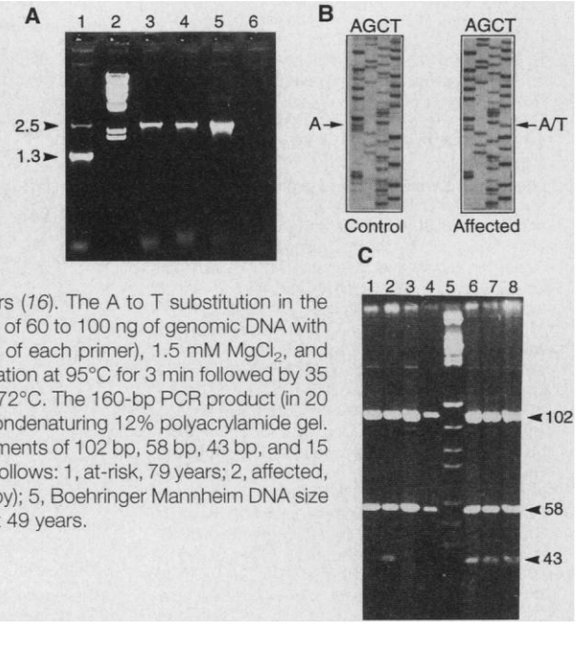

Fig. 2. Mapping, DNA sequence analysis of AD4, and Sau 3A mutation detection. (**A**) Polymerase chain reaction primers were designed from T03796 to yield a 188-bp product from a T03796-equivalent cDNA clone (primers WWF and WWR) (*11*). Amplification of genomic DNA produced a strong 1.3-kb band and a faint 2.5-kb band (markers on left) (lane 1). The 1.3-kb band was sequenced and did not contain the EST sequence. The 60 chromosome 1 YACs (*8*) were initially screened by PCR with primers EP1F and EP1R (*3*) and subsequently with primers WWF and WWR; a single YAC (921D12) yielded a strong 2.5-kb product with both primer pairs. The three largest subclones of 921D12 (lanes 3 to 5) contained the 2.5-kb fragment, whereas the smallest clone (lane 6) did not (*12*). Lane 2 contains Lambda Hind III molecular weight standards. (**B**) DNA sequence analysis of RT-PCR products from an affected VG subject and a control. RT-PCR products were amplified with primers 5′-GATCGTGGTGGTAGCCACCA-3′ (nt 664 to 683) and 5′-TCCCAGACAGTCAGCAAGAG-3′ (nt 995 to 977) (*14*) and sequenced with the same primers (*16*). The A to T substitution in the affected person is the N1411 mutation. (**C**) The N141I mutation is detected by amplification of 60 to 100 ng of genomic DNA with primers WWF (*11*) and INT1R (intronic primer 5′-GTGGGGCAGACGGAGAGAA-3′, 40 ng of each primer), 1.5 mM $MgCl_2$, and deoxynucleotide triphosphates (200 μM). Amplification was performed with an initial incubation at 95°C for 3 min followed by 35 cycles of 45 s at 94°C, 45 s at 60°C, and 45 s at 72°C, with a final incubation for 10 min at 72°C. The 160-bp PCR product (in 20 μl) was digested with 10 U of Sau3A and the fragments resolved by electrophoresis in a nondenaturing 12% polyacrylamide gel. Fragments were visualized by ethidium bromide staining. The N141I mutation results in fragments of 102 bp, 58 bp, 43 bp, and 15 bp (not shown), whereas noncarriers have only the 102- and 58-bp fragments. Lanes are as follows: 1, at-risk, 79 years; 2, affected, onset 60 years; 3, at-risk, 67 years of age; 4, affected, onset 75 years (presumed phenocopy); 5, Boehringer Mannheim DNA size standard V; 6, affected, onset 52 years; 7, affected, onset 46 years; and 8, affected, onset 49 years.

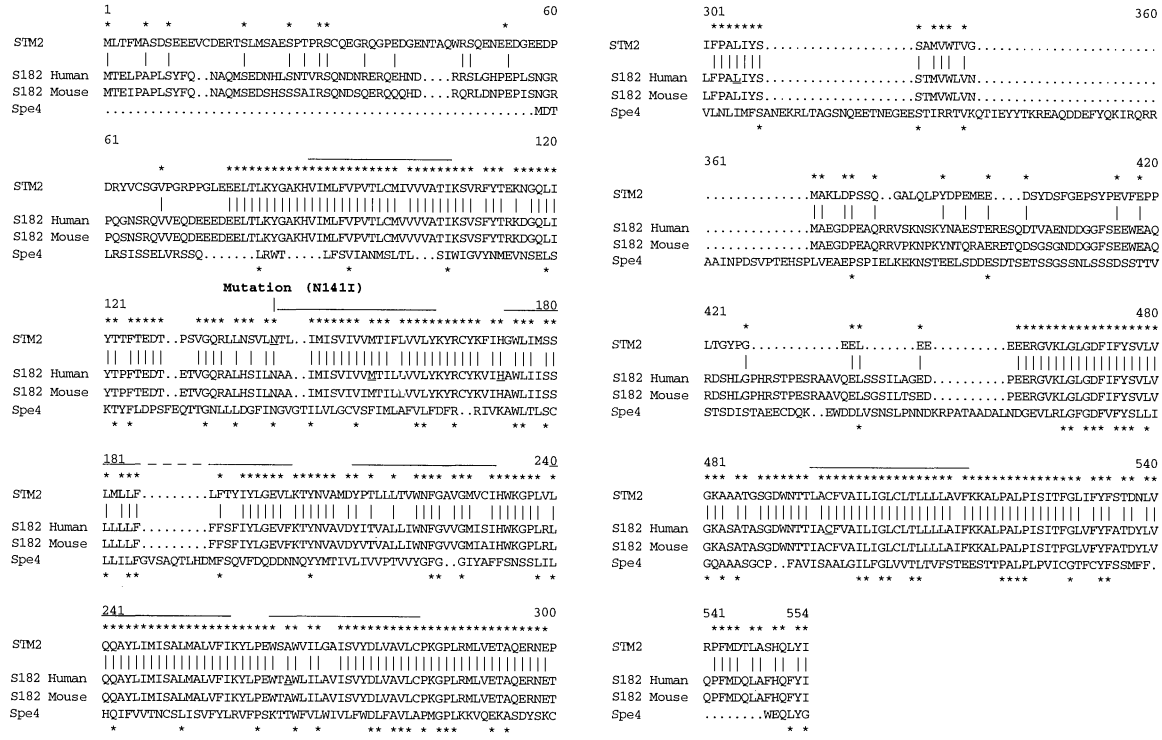

Fig. 3. Alignment of the protein sequence of STM2 with the chromosome 14 AD3 gene product, S182, for humans and mice, and the Spe4 protein from *C. elegans*. The coordinates indicated are not for any one of the aligned sequences. The N141I mutation, for example, is at position 141 of STM2, but at position 143 of the alignment. The asterisks at the top of the alignment indicate matches in the upper three proteins, whereas the asterisks at the bottom indicate matches over all four of the sequences. Exact matches between the STM2 and S182 proteins are also indicated. The position of the N141I mutation is shown, and the positions of the five reported mutations in S182 (*2*) are indicated as underlined letters in the normal sequence. The seven putative TMDs are indicated by lines at the top of the alignment. Abbreviations for the amino acid residues are: A, Ala; C, Cys; D, Asp; E, Glu; F, Phe; G, Gly; H, His; I, Ile; K, Lys; L, Leu; M, Met; N, Asn; P, Pro; Q, Gln; R, Arg; S, Ser; T, Thr; V, Val; W, Trp; and Y, Tyr.

the 112-bp allele of D1S479 (allele H in Fig. 1) was observed in most affected people in five of seven VG families (*4*) and is potentially in linkage disequilibrium with the chromosome 1 AD gene.

We cloned the gene corresponding to T03796, designated F (full-length) T03796, by screening human brain and fibroblast complementary DNA (cDNA) libraries with a probe derived from the EST sequence (*13*). Clones of approximately 2.3 kb were obtained from both cDNA libraries. Sequence analysis of one brain and two fibroblast clones (*14*) showed that each contained the T03796 sequence and had a 448–amino acid open reading frame (GenBank accession number L43964) that was closely homologous to S182 (Fig. 3). Northern (RNA) blot analysis of RNA from a variety of human tissues revealed two F-T03796–related transcripts that were approximately 2.4 and 2.8 kb in size (*15*). The larger transcript appears to be primarily expressed in placenta, skeletal muscle, and heart, whereas the smaller transcript is detected in heart, brain, placenta, liver, skeletal muscle, and kidney, but not lung. A sequence-tagged site (STS) from the 3′ untranslated region was used to confirm that F-T03796 maps to chromosome 1 and to YAC 921D12 (*11*).

The entire coding region of the F-T03796 gene was screened for mutations in four affected VG subjects from the HB, HD, R, and W families (*16*). The affected people were heterozygous at codon 141 (AAC/ATC), which results in the substitution of an isoleucine for an asparagine (N141I) (Fig. 2B). The substitution creates a Sau 3A restriction site that permits rapid genotyping of the N141I mutation (Fig. 2C). Affected people carrying the N141I mutation were identified in five (H, HB, HD, R, and W) of the seven VG families initially screened. All people with the N141I mutation also carried the D1S479 112-bp allele (allele H, Fig. 1). Subsequently, two additional VG families (E and BE) were screened for the N141I mutation. These families had not been used in the linkage study (*4*) because DNA was available from only one affected (BE family) or one possible AD subject (E family). In both kindreds, the affected people carried the N141I mutation and the D1S479 112-bp allele. In total, the N141I mutation was directly observed in 20 affected subjects and was inferred to be present from spouse-children genotypes in an additional six AD subjects; ages of onset for the 26 people ranged from 44 to 75 years. The N141I mutation was also observed in 15 at-risk subjects (blood relatives of affected N141I carriers), with ages ranging from 23 to 67 years. No VG spouse (n = 17) had the N141I mutation. Additional populations screened included 84 normal Caucasians, spouses, at-risk subjects, and affected subjects from 67 late-onset familial FAD families (n = 223 affected people), and 48

Table 1. Lod scores for linkage of N141I to AD. For the APOE covariate sporadic model, a mean onset of 80 was used for sporadic APOE ϵ4/ϵ4 cases. For all gene frequencies examined, the likelihood maximized at an ϵ4/ϵ4 mean onset of 81. These results are quite insensitive to assumptions about the N141I mutation frequency (over a range of 0.0001 to 0.015) and the ϵ4/ϵ4 mean onset age (over a range of 70 to 100 years): the highest lod score was 8.51 at a gene frequency of 0.0001 and an ϵ4/ϵ4 mean onset of 81 years, whereas the lowest was 8.04 at a gene frequency of 0.015 and a mean ϵ4/ϵ4 onset of 100 years. $\hat{\theta}$ indicates the recombination fraction at which Z_{max} was obtained.

Model	Lod scores for recombination fraction (θ)								Z_{max} ($\hat{\theta}$)
	0.0	0.001	0.05	0.10	0.15	0.20	0.30	0.40	
Age-dependent penetrance	2.04	3.11	5.89	5.92	5.56	4.98	3.47	1.68	5.97 (0.08)
General sporadic	7.91	7.90	7.50	6.90	6.18	5.38	3.60	1.68	7.91 (0.0)
APOE covariate sporadic	8.35	8.34	7.88	7.22	6.45	5.60	3.73	17.4	8.35 (0.0)

affected sporadic people from an AD clinic population. No other N141I mutation carriers were identified (*17*).

No one in the KS or WFL families had the N141I mutation. These two families are thought to represent genetic heterogeneity within the VG families for the following reasons. (i) Neither family had previously yielded positive linkage evidence to chromosome 1 markers. (ii) Affected members of these families did not share the same haplotype as observed in affected members of other VG families (*4*) (Fig. 1). (iii) The age of onset is higher for the WFL and KS kindreds compared to other VG families (Fig. 1). In the seven families in which most of the affected subjects had the N141I mutation (BE, E, H, HB, HD, R, and W), there were two affected subjects (one in the R family and one in the HD family) who did not have the N141I mutation. The HD subject had onset of AD at 75 years of age and was APOE ϵ3/ϵ4, and the R subject had onset of AD at 67 years and was an APOE ϵ4/ϵ4 homozygote. Neither had the 112-bp D1S479 allele that segregates with the major AD gene in the VG families (*4*) (Fig. 1).

To evaluate the evidence that the nonmutation carriers may be phenocopies, logarithm of the likelihood ratio for linkage (lod) scores for linkage of N141I to AD in the seven VG families (H, HB, HD, KS, W, and WFL) were computed under three models (*18*) (Table 1). Results from the standard age-corrected penetrance method were compared to lod scores computed with two different phenocopy correction models. The general sporadic correction model assumes that the probability that a subject is a phenocopy increases with age of onset. The APOE covariate sporadic model adds the assumption that APOE ϵ4/ϵ4 sporadic subjects have an earlier age of onset than non-ϵ4/ϵ4 sporadic subjects. Both phenocopy correction models yielded higher values for the peak lod score (Z_{max}) compared to the standard model, with the highest value obtained from the APOE-covariate sporadic model (Table 1). Also, for both phenocopy correction models, maximum lod scores were at 0% recombination, as compared to 8% for the standard model. Accurate specification of parameters in a genetic model generally produces lower and more accurate estimates of the recombination fraction and higher lod score estimates when compared to results from models where inaccurate parameters are used (*19*). Thus, these results support the hypothesis that there are phenocopies in the VG pedigrees, particularly subjects who are APOE ϵ4/ϵ4. This interpretation is further supported by the fact that non-N141I carrier AD subjects appear to have a higher age of onset compared to N141I carriers (mean = 66 years, n = 11, range = 57 to 75 versus mean = 54 years, n = 26, range = 44 to 75, respectively). Also, noncarriers had a higher ϵ4 allele frequency (0.59, n = 22 alleles) compared to carriers (0.19, n = 46 alleles).

The amino acid sequence predicted by F-T03796 exhibits similarity to S182 (*2*) (Fig. 3). At the amino acid level, the two genes were 67% identical. A similar degree of homology was found between the chromosome 1 gene and the mouse S182 homolog; the three mammalian genes also displayed similarity to the *Caenorhabditis elegans spe4* gene (*20*). The N141I mutation reported here and all five mutations reported in S182 (*2*) occur at residues conserved between the chromosome 1 gene, S182, and the mouse S182 homolog. Like S182 and *spe4*, hydropathy plots from the F-T03796 sequence predict that the encoded protein has seven transmembrane domains and is thus referred to as STM2 (the second seven transmembrane gene associated with AD). Within the putative transmembrane domains (TMDs), the sequence similarity between STM2 and S182 is striking, with an identity of 84%. For STM2, all the putative transmembrane helices are capped at the COOH-terminal end by a lysine residue, found either at the very end or within a few residues of the end of the TMDs. The N141I mutation constitutes a change from a hydrophilic asparagine residue to a hydrophobic isoleucine residue at a position directly adjacent to the first predicted TMD (Fig. 3). Likewise, one of the reported S182 familial AD mutations occurs immediately before a putative TMD and three others occur within the first three residues of predicted TMDs. These mutations may all, therefore, adversely affect the insertion or anchoring of these proteins in membranes. The non-TMD regions show less conservation between STM2 and S182; the regions of greatest divergence are the 80 amino acids at the NH_2-terminal end and the sequence in the hydrophilic loop between the sixth and seventh TMD. In this latter region, STM2 is shorter than S182 by 24 residues.

The normal cellular functions of STM2 and S182 are unknown. If these proteins are functionally similar to those encoded by *spe4*, potentially functioning in the cytoplasmic partitioning of proteins, mutations in S182 and STM2 could alter intracellular protein trafficking of APP and ultimately lead to altered APP processing and increased production of amyloid precursor proteins $A\beta_{1-40}$ or $A\beta_{1-42}$. Consistent with this idea, recent work with fibroblast cell lines from AD3 carriers has shown that secretion of Aβ ending at position 42 is increased relative to noncarrier cell lines (*21*). It is also conceivable that the STM2 and the S182 gene products may function as G protein–coupled receptors or as ion channels.

REFERENCES AND NOTES

1. A. M. Goate *et al.*, *Nature* **349**, 704 (1991); M. H. Chartier-Harlin *et al.*, *ibid.* **353**, 844 (1991); J. Murrell, M. Farlow, B. Ghetti, M. D. Benson, *Science* **254**, 97 (1991); M. Mullan *et al.*, *Nature Genet.* **2**, 340 (1992).
2. R. Sherrington *et al.*, *Nature* **375**, 754 (1995).
3. E. H. Corder *et al.*, *Science* **261**, 921 (1993).
4. E. Levy-Lahad *et al.*, *ibid.* **269**, 970 (1995).
5. F. C. Koch, *The Volga Germans* (Pennsylvania State Univ. Press, University Park, PA, 1977); R. D. Scheuerman and C. E. Trafzer, *The Volga Germans: Pioneers of the Northwest* (University Press of Idaho, Moscow, ID, 1985).
6. R. Cook *et al.*, *Neurology* **29**, 1402 (1979); T. D. Bird *et al.*, *Ann. Neurol.* **23**, 25 (1988); T. D. Bird *et al.*, *ibid.* **25**, 12 (1989); T. D. Bird, *J. Am. Histo. Soc. Germ. Russia* **49**, 1 (Fall 1991); T. D. Bird *et al.*, *Heterogeneity of Alzheimer's Disease*, F. Boller *et al.*, Eds. (Springer-Verlag, Heidelberg, 1992), pp. 118–129; G. D. Schellenberg *et al.*, *Science* **241**, 1507 (1988); G. D. Schellenberg *et al.*, *Am. J. Hum. Genet.* **48**, 563 (1991); G. D. Schellenberg *et al.*, *ibid.* **49**, 511 (1991); K. Kamino *et al.*, *ibid.* **51**, 998 (1992); G. D. Schellenberg *et al.*, *Science* **258**, 668 (1992).
7. G. D. Schellenberg *et al.*, *Am J. Hum. Genet.* **53**, 619 (1993).
8. The Centre d'Etude du Polymorphisme Humain (CEPH)–Genethon YAC database was queried with loci D1S229, D1S227, D1S213, D1S479 D1S439, D1S225 D1S103, and D1S459; 58 YACs were identified either as having the marker or as being adjacent to the query marker. For D1S320 and D1S479, the CEPH-Genethon library, arrayed for polymerase chain reaction (PCR) screening, was screened directly with the published primer sets for these markers. One YAC for each marker was identified.
9. T. Azuma, W. Liu, D. J. Vander Lann, A. M. Bowcock, R. T. Taggart, *J. Biol. Chem.* **267**, 1609 (1992).
10. H.-G. Bernstein and B. Wiederanders, *Brain Res.* **667**, 287 (1994); N. Nakanishi *et al.*, *Exp. Neurol.* **121**, 215 (1993).
11. DNA from YAC 921D12 was amplified with primers WWF (5′-GGACACACCCTCGGTGGGCC-3′ [from nucleotide (nt) 745 to 764] and WWR 5′-CAAGGTAGATATAGGTGA-3′ (nt 943 to 925) to produce the 2.5-kb band shown in Fig 2A. This band was gel-purified and sequenced directly with the same primers. The sequence contained 119 bp of the T03796 sequence on one end separated, presumably by intronic sequence, from 69 bp of T03796 sequence at the other end. The sequence obtained was used to design two intronic primers (921D12F, 5′-TCCAGCCACCCTTCTCTCC-3′; 921D12R, 5′-ACAGTATTAGGTCATCCACGGT-3′). PCR amplification of genomic DNA with these primers produced a 154-bp STS. Primers were also designed from the 3′ untranslated region of F-T03796 [ADC22L5, 5′-GGGACATGGTGTGCCACAG-3′ (nt 1715 to 1733); DMO1009, 5′-ACAGGACTCATCTATTTATTGATA-3′ (nt 2228 to 2205)], which produce a 519-bp fragment from genomic DNA. When either set of primers was used to amplify DNA from the Coriell Institute for Medical Research hybrid mapping panel number 2, the appropriate 154-bp or 519-bp fragment was observed only in the cell line containing chromosome 1 as the sole human chromosome.
12. Four separate subclones of YAC clone 921D12 were analyzed for size and marker content. The largest clone (>1600 kb) contained D1S439, D1S479, D1S1644, and T03796 (*11*). The other three subclones were smaller (1280, 1280, and 800 kb) and contained only a subset of these loci.
13. We obtained the cDNA clones corresponding to T03796 by screening a human fibroblast cDNA library, prepared from a patient with Werner's syndrome, and cloned them in Lambda ZAP pKB-CMV (Stratagene) and a human brain frontal cortex Lambda Zap II cDNA library (Stratagene). The fibroblast library was screened by plaque hybridization with a 140-bp probe produced by amplification of a portion of the pooled fibroblast library with primers EP1F and EP1R [5′-CTTGGTGGTGCTCTACAAGTAC-3′ (nt 832 to 853) and 5′-GTAGTCCATGGCCACATTGT-3′ (nt 970 to 951)]. Four clones were obtained, and two were characterized further; clone PP15A was

2.3 kb and clone PP11 was 1.9 kb. The same fibroblast library, arrayed for PCR screening [D. J. Munroe *et al.*, *Proc. Natl. Acad. Sci. U.S.A.* **92**, 2209 (1995)], was screened with EP1R and EP1F primers; a single clone (PPc11) was characterized and found to be 2.3 kb. The brain library was screened by plaque hybridization by conventional methods [J. Sambrook, E. F. Fritsch, T. Maniatis, *Molecular Cloning: A Laboratory Manual* (Cold Spring Harbor Laboratory, Cold Spring Harbor, NY, 1989)] with the use of a 192-bp probe produced by amplification of a human lymphoblast cDNA library with the use of primers [5′-TCACTGAGGACACACCCTCG-3′ (nt 738 to 757) and 5′-GGTAGATATAGGTGAAGAGG-3′ (nt 929 to 910)] complementary to T03796. Three clones were obtained from the brain library: PS2-41 (2.3 kb), PS2-6 (1.9 kb), and PS2-10 (1.7 kb).

14. Three fibroblast cDNA clones (PPc11, PP15A, and PP11) were sequenced as follows. The cDNA fragments in pBK-CMV (Stratagene) were excised from agarose gels, purified with a Gene-Clean kit (Bio-101), and fragmented by flow extrusion in high-performance liquid chromatography (P. Oefner, personal communication) to a size range of 0.5 to 1 kb. These fragments were cloned directly into M13mp18 (Novagen) cut by Sma I and phosphatased with the use of the manufacturer's protocols. The resulting plaques were picked into PCR buffer and amplified with primers homologous to the vector. The PCR products were purified on a G-50 spin column and sequenced with Applied Biosystems forward and reverse dye-primer sequencing kits. Samples were run on an Applied Biosystems 373 A sequencer. The data were assembled with DNAStar, with the translated coding region shown in Fig. 3. Three brain cDNA clones (PS2-41, PS2-6, and PS2-10) were sequenced manually with Sequenase from U. S. Biochemical. The DNA sequence has been deposited in GenBank (accession number L43964). The nucleotide numbering used here is based on the ATG codon being at nt 368 to 370.
15. A Northern blot (Clontech) containing 2 μg of human polyadenylated mRNA derived from heart, brain, placenta, lung, liver, skeletal muscle, and pancreas was hybridized with the 2.3-kb F-T03796 cDNA clone as a probe. Hybridization was in 0.75 M NaCl, 0.05 M NaH_2PO_4, 5 mM Na_2EDTA, ×10 Denhardt's solution, 100 μg/ml salmon sperm DNA, 50% formamide, and 2% SDS at 42°C for 18 hours. Filters were washed with ×0.1 saline sodium citrate and 0.1% SDS at 65°C. The two transcripts observed are possibly the result of alternative polyadenylation because two putative polyadenylation signals were identified in the 3′ untranslated region, starting at nucleotides 1834 and 2309 (*14*). The message sizes for STM2 from Northern blot analysis (2.4 and 2.8 kb) were larger than the 2.3-kb size predicted from the full-length DNA sequence and the 1.8-kb size predicted by the second polyadenylation site observed in that sequence. This discrepancy is possibly due to the anomalous migration of size markers that has been previously observed with this type of Northern blot.
16. Reverse transcription (RT)–PCR products synthesized from RNA (Becton Dickinson Mini RiboSep) prepared from affected VG subjects and controls were amplified with a variety of primers and the PCR products cycle-sequenced with the Promega fmol DNA Sequencing System. In other experiments, RT-PCR products were gel-purified, re-amplified with the same primers, and sequenced with a U.S. Biochemicals Sequenase PCR Product sequencing kit. In addition to the N141I mutation, three sequence variants were identified at nucleotides 436 (C/T, HB subject), 496, (C/T, HD and W subjects), and 628 (C/T, HD and W subjects). These variants did not change the amino acid encoded at these sites (alanine, asparagine, and histidine, respectively).
17. An upper confidence bound on the mutation gene frequency, p, when no mutations are found, can be found with the equation $(1 - p)^N = \alpha$, where N is the number of chromosomes tested and α is the desired significance level. A 95% upper confidence limit for the N141I mutation frequency is 0.0077, based on no mutations observed in 195 independent controls.
18. Lod scores for the age-dependent penetrance model were computed as described (*4*). For the general sporadic model, the program LIPED was modified to correct for phenocopies (*7*) caused by possible sporadic AD by taking actual age of onset into account [P. Margaritte *et al.*, *Am. J. Hum. Genet.* **50**, 1231 (1992)] and with the assumption of a mean sporadic onset age of 110 years and a standard deviation of 20 years. We obtained these values for the sporadic rate by maximizing the likelihood of the data in the presence of linkage to D1S479 (*4*). For the covariate sporadic model, an additional modification to LIPED allowed use of the APOE genotype as a covariate, so that the APOE ε4/ε4 genotype was assumed to have a lower sporadic mean onset than the general population sporadic onset. An AD allele frequency of 0.001, a N141I allele frequency of 0.0077, and a mean sporadic onset age for APOE ε4/ε4 ranging in 5-year increments from 70 to 100 were used.
19. F. C. Clerget-Darpoux, C. Bonaiti-Pellie, J. Hochez, *Biometrics* **42**, 393 (1986).
20. S. M. L'Hernault and P. M. Arduengo, *J. Cell Biol.* **119**, 55 (1992).
21. D. Scheuner, *et al.*, *Soc. Neurosci. Abstr.*, in press; X.-H. Song *et al.*, *ibid.*, in press.
22. Supported by grants from the National Institute on Aging for the Alzheimer's Diseases Research Center at the University of Washington (AG0513C) and grants RO1-AG11762 (G.D.S.) RO1-AG11899 (W.W.), and RO1-NS30428 (R.E.T.), Veterans Affairs Research Funds, and National Research Service Award postdoctoral fellowship F32 AG05635 (E.L.-L.), the American Health Assistance Foundation (G.D.S. and R.E.T.), the French Foundation (R.E.T.), and an American Physicians Fellowship (E.L.-L.). W.W. is a Becton-Dickinson Fellow and R.E.T. is a Pew scholar in Biomedical Sciences. We thank D. Nochlin, M. Sumi, M. Ball, and G. Glenner for neuropathologic characterization of many of the families, A. Lahad for statistical consultations, E. Loomis, L.-J. Anderson, E. Jeffrey, B. Paeper, T. Britschgi, L. Gordon, and R. Alish for technical help, H. Lipe and T. Lampe for obtaining blood samples and medical records, M. Boehnke and A. Motulsky for reading the manuscript before publication, J. Mulligan for much help and advice, M. Brunkow for helpful discussion, and R. Jones for help in the sequence analysis. Informed consent was obtained from each subject or next of kin with approval of the University of Washington Human Subjects Review Committee. We also thank the many family members who generously cooperated in this study, the American Historical Society of Germans from Russia, and T. Kloberdanz, G. Miner, and R. Cook-Deegan.

17 July 1995; accepted 24 July 1995

Ionic Mechanisms of Neuronal Excitation by Inhibitory $GABA_A$ Receptors

Kevin J. Staley,* Brandi L. Soldo,† William R. Proctor

Gamma-aminobutyric acid A ($GABA_A$) receptors are the principal mediators of synaptic inhibition, and yet when intensely activated, dendritic $GABA_A$ receptors excite rather than inhibit neurons. The membrane depolarization mediated by $GABA_A$ receptors is a result of the differential, activity-dependent collapse of the opposing concentration gradients of chloride and bicarbonate, the anions that permeate the $GABA_A$ ionophore. Because this depolarization diminishes the voltage-dependent block of the *N*-methyl-D-aspartate (NMDA) receptor by magnesium, the activity-dependent depolarization mediated by GABA is sufficient to account for frequency modulation of synaptic NMDA receptor activation. Anionic gradient shifts may represent a mechanism whereby the rate and coherence of synaptic activity determine whether dendritic $GABA_A$ receptor activation is excitatory or inhibitory.

Transient decreases in inhibition are necessary for the induction of plasticity at Hebbian synapses (*1*). High-frequency stimulation, which mimics the in vivo firing frequencies of the interneurons that release GABA (*2*), is the most robust method of increasing synaptic strength (*1*). $GABA_A$ receptor activation, which is normally inhibitory (*3*), becomes excitatory at these high frequencies because the postsynaptic membrane is depolarized rather than hyperpolarized (*4*–*6*). The mechanism of this depolarization is unknown but should involve the flux of chloride (Cl^-) and bicarbonate (HCO_3^-) because the $GABA_A$ ionophore is selectively permeable to these anions (*7*, *8*). Although some classes of neurons maintain a resting Cl^- reversal potential (E_{Cl}) that is more positive than the resting membrane potential (RMP) (*3*, *9*, *10*), in neurons such as pyramidal cells that maintain E_{Cl} negative to the RMP, regional (*11*) and activity-dependent (*12*) differences in the cytoplasmic Cl^- concentration ($[Cl^-]_i$) are not sufficient to explain the activity-dependent $GABA_A$ receptor–mediated depolarization (*13*, *14*). The HCO_3^- reversal potential (E_{HCO_3}) is much more positive than the RMP (*15*), but efforts to define a role for HCO_3^- in the GABA-mediated depolarization have been inconclusive (*16*), as it has not been possible to reconcile a depolarizing HCO_3^- efflux with the salient characteristics of the GABA-mediated depolarization: activity dependence, slow kinetics, and dendritic localization (*4*–*6*).

K. J. Staley, Departments of Neurology and Pediatrics B182, University of Colorado Health Sciences Center, 4200 East 9th Avenue, Denver, CO 80262, USA.
B. L. Soldo and W. R. Proctor, Department of Pharmacology, University of Colorado Health Sciences Center, and Denver VA Medical Center, Denver, CO 80262, USA.

*To whom correspondence should be addressed.
†Present address: Department of Physiology, University of Michigan Medical School, Ann Arbor, MI 48109, USA.